

Adaptive Wavelet Packet Basis Selection for Zerotree Image Coding

Nasir M. Rajpoot, *Member, IEEE*, Roland G. Wilson, François G. Meyer, *Member, IEEE*, and Ronald R. Coifman

Abstract—Image coding methods based on adaptive wavelet transform and those employing zerotree quantization have been shown to be successful in recent years. In this paper, we present a general zerotree structure for an arbitrary wavelet packet geometry in an image coding framework. A fast basis selection algorithm which uses a Markov chain based cost estimate of encoding the image using this structure is developed. As a result, our adaptive wavelet zerotree image coder has a relatively low computational complexity, performs comparably to the state-of-the-art image coders, and is capable of progressively encoding images.

Index Terms—Basis selection, image coding, wavelet transform, zerotree quantization.

I. INTRODUCTION

THE development of image coding systems which can produce visually pleasing results at low bit rates has been an active branch of image processing for more than three decades now. The study of the human visual system (HVS) has played an important role in this work, largely because spatial frequency subband decomposition appears to be a key feature of the HVS [3]. Early subband image coding methods, such as [1], [28], were motivated by this observation. The development of wavelets by Strömberg [23] in 1981 and the work by Mallat and Meyer [12], [13] in 1987 led to a surge of research in wavelet transform based image coding, partly due to the fact that the wavelet transform closely matches the feature of the HVS mentioned above¹ [13].

Wavelet based *zerotree* image coding methods [21], [22] exploit the similarities across wavelet subbands by grouping coefficients belonging to subbands of different resolutions and encoding the group as a single codeword. The zerotree coding schemes are quite efficient in terms of both computational complexity and compression performance. Moreover, embedded (progressive) transmission (reconstruction), which is required in many applications, using zerotrees with successive approximation quantization (SAQ), is quite straightforward. Wavelet

based methods, however, have a problem at low bit rates: while they perform well on images containing smooth regions and edges, they perform poorly on images with oscillatory patterns, such as the *Barbara* image (Fig. 18). The quantization of many low energy coefficients belonging to the high frequency subbands causes artificial smooth regions (*smearing*) in the areas of the image that contain rapid variations of intensity.

Wavelet packets were invented [4] to pinpoint signal components present locally in the frequency domain. The nondyadic nature of a wavelet packet (WP) transform allows us to find an orthogonal basis adapted to the contents of given image and to the purpose of representation. However, there has not been as much research activity in wavelet packet image coding as in the area of wavelet image coding, due to its being computationally more expensive than the wavelet transform.

In this paper, we explore the possibility of wedding the adaptive wavelet packet transform with zerotree quantization. To the best of our knowledge, the only wavelet packet image coding algorithms found in the literature that employ zerotree quantization, partially or fully, are [30] and [2]. The rearrangement algorithm of Cho and Ra [2] puts together the coefficients of four split subbands to merge them back into a single subband, as if no split was made. This rearrangement is iterated until a wavelet-like subband decomposition is obtained. The SPIHT coder is then applied to this wavelet-like decomposition. However, this algorithm faces the following consistency problem: after the rerearrangement, four child coefficients of a coefficient in a lower frequency subband do not necessarily belong to the same spatial location. The issue of wavelet packet zerotrees was also addressed partially in the space-frequency quantization (SFQ) algorithm of Xiong *et al.* [30], which employs a rate-distortion (R-D) optimization framework to select the best basis and to assign an optimal quantizer to each of the wavelet packet subbands. In their work, however, the subband decomposition was restricted to avoid the *parenting conflict*, a problem explained in Section III-B, a constraint which may result in the selection of a suboptimal basis. Moreover, the computational complexity of the SFQ algorithm is quite high: according to the authors [30], the overall complexity of their practical wavelet coder using the suboptimal heuristic is the sum of the complexities of [19] and [29].

The following questions are addressed in this paper: 1) Can the zerotree quantization strategy be applied to the wavelet packet transformed images? 2) If so, how can the spatial orientation trees, or zerotrees, be defined in order to predict the insignificance of corresponding wavelet packet coefficients, given a parent coefficient? 3) Is there an efficient way of selecting the best basis adapted to both image contents and the

Manuscript received December 12, 2002; revised May 25, 2003. The associate editor coordinating the review of this manuscript and approving it for publication was Dr. Fernando M. B. Pereira.

N. M. Rajpoot and R. G. Wilson are with the Department of Computer Science, University of Warwick, Coventry CV4 7AL, U.K. (e-mail: nasir@dcs.warwick.ac.uk; rgw@dcs.warwick.ac.uk).

F. G. Meyer is with the Department of Electrical Engineering, University of Colorado at Boulder, 80309 USA (e-mail: francois.meyer@colorado.edu).

R. R. Coifman is with the Department of Mathematics, Yale University, 06520 USA (e-mail: coifman@math.yale.edu).

Digital Object Identifier 10.1109/TIP.2003.818115

¹In general, harmonic analysis, *the study of harmonic components of a given signal*, has had an enormous impact on the evolution of present day image coding techniques (for a detailed exposition on the topic; see [8]).

purpose of representation, i.e., encoding by zerotree quantization? The validity of the first of these questions arises from the fact that there is less self-similarity among the wavelet packet subbands than among the wavelet subbands. We first provide an answer to 2), assuming that zerotree quantization can be applied to the wavelet packet decomposition of an image. A generalized zerotree structure termed the *compatible zerotree* structure, which provides a quantization framework for encoding the wavelet packet coefficients, is presented. The answer to 1) becomes clear from the successful testing of this structure and the coding results. In addressing 3), we suggest a fast way of estimating the cost of compatible zerotree quantization. This cost estimation function enables us to present an efficient basis selection algorithm resulting in a *zerotree friendly* basis.

This paper is organized as follows. The next section gives a brief review of both fixed and adaptive wavelet transforms. The idea of zerotrees is extended from wavelet zerotrees to compatible zerotrees for wavelet packets in Section III, and rules for generating the compatible zerotrees are presented. In Section IV, the hypothesis that the significance of child coefficients in a compatible zerotree can be predicted by knowing the significance of the parent coefficient is described and tested. A Markov chain based cost function that allows us to efficiently select the best basis is given in Section V. The coding algorithm and experimental results are presented in Section VI. The paper concludes with a summary and discussion of results.

II. ADAPTIVE WAVELET TRANSFORM

A. Introduction

The introduction of multiresolution image representations has been one of the most important developments in image analysis and coding over the last two decades [1], [11], [20], [24], [26], [27]. The idea of analyzing a signal locally at different scales has resulted in a multidisciplinary boom in research on wavelets, attracting researchers from many different branches of science [7], [9], [13], [16]. The principle behind wavelets is that shifts and dilations of a prototype function $\psi(t)$, also known as the *mother wavelet function*, are chosen as basis functions to represent a signal, while the scaling function $\phi(t)$ is used to approximate the function at different scales. In the case of the wavelet transform of a signal f of length N , the approximation space V_j of the signal at a resolution 2^{-j} is decomposed into a lower resolution space V_{j+1} and a detail space W_{j+1} . This is done by dividing the orthogonal basis $\{\phi_j(t - 2^j n)\}_{n \in \mathcal{Z}}$ of V_j into two bases $\{\phi_{j+1}(t - 2^{j+1} n)\}_{n \in \mathcal{Z}}$ of V_{j+1} and $\{\psi_{j+1}(t - 2^{j+1} n)\}_{n \in \mathcal{Z}}$ of W_{j+1} , where $\phi_j(t) = 2^{-j/2} \phi(2^{-j} t)$ and $\psi_j(t) = 2^{-j/2} \psi(2^{-j} t)$, using lowpass and highpass filters $h[n]$ and $g[n]$, respectively, in a two-channel filter bank.

A more general form of the wavelet basis, known as the *wavelet packet basis* [4], [5], adaptively segments the frequency axis. Frequency intervals of varying widths are adaptively selected to extract the frequency content present in the given signal. In order to approximate the signal f belonging to an approximation space $V_j = W_j^0$ at a resolution 2^{-j} using wavelet packets, the space W_j^0 is decomposed into two orthogonal spaces W_{j+1}^0 and W_{j+1}^1 . Each of these spaces can be further decomposed into two orthogonal spaces. In general, Coifman and

Meyer [4] proved that if $\{\psi_j^p(t - 2^j n)\}_{n \in \mathcal{Z}}$ is an orthonormal basis of W_j^p , where $W_j^0 = V_j$, $W_j^1 = W_j$ and $\psi_j^0 = \phi_j$, $\psi_j^1 = \psi_j$, then $\{\psi_{j+1}^{2p}(t - 2^{j+1} n), \psi_{j+1}^{2p+1}(t - 2^{j+1} n)\}_{n \in \mathcal{Z}}$ is also an orthonormal basis of W_j^p , where

$$\psi_{j+1}^{2p}(t) = \sum_{n=-\infty}^{+\infty} h[n] \psi_j^p(t - 2^j n) \quad (1)$$

$$\psi_{j+1}^{2p+1}(t) = \sum_{n=-\infty}^{+\infty} g[n] \psi_j^p(t - 2^j n), \quad (2)$$

and $W_j^p = (W_{j+1}^{2p} \oplus W_{j+1}^{2p+1})$. The discrete wavelet packet transform (DWPT) of a one-dimensional (1D) discrete signal \mathbf{x} of length N can be computed as follows [4],

$$\begin{aligned} w_{2n,d,l} &= \sum_k g_{k-2l} w_{n,d-1,k} & l = 0, 1, \dots, N2^{-d} - 1 \\ w_{2n+1,d,l} &= \sum_k h_{k-2l} w_{n,d-1,k} & l = 0, 1, \dots, N2^{-d} - 1 \\ w_{0,0,l} &= x_l & l = 0, 1, \dots, N - 1 \end{aligned} \quad (3)$$

where $d = 1, 2, \dots, J - 1$; $J = \log_2 N$, $w_{n,d,l}$ is the transform coefficient corresponding to the wavelet packet function which has relative support size 2^d , frequency $n2^{-d}$ and is located at $l2^d$. In other words, d , n and l can be regarded respectively as the scale, frequency and position indices of the corresponding wavelet packet function. The coefficients $\{h_n\}$ and $\{g_n\}$ correspond to the lowpass and highpass filters respectively for a two-channel filter bank and the transform is invertible if appropriate dual filters $\{\tilde{h}_n\}$, $\{\tilde{g}_n\}$ are used on the synthesis side. The DWPT can be regarded as a decomposition which removes the constraint of only decomposing the lowpass filtered signal, so that all subbands can be further decomposed. This results in a combinatorial explosion of possible bases from which to select a suitable basis. Since this library of available bases provides an overcomplete description, a fast optimization algorithm is required to select a basis from this library.

B. Number of Possible Bases

Following the notation of [14], a *wavelet packet tree* for a 1D signal is a tree which (1) has the original signal as its root node λ_0^0 and (2) each of the two sibling nodes elsewhere in the tree represent two subbands λ_d^{2n} and λ_d^{2n+1} resulting from the decomposition (or split) of their parent node λ_{d-1}^n . There can be 2^d nodes at a depth d of the wavelet packet tree in the case of a 1D signal. This makes a total of $2^{J+1} - 1$ nodes in a wavelet packet tree of maximum depth J . The binary nature of this wavelet packet tree suggests that the number of possible bases N_d at a depth d satisfies the following relation

$$N_d = N_{d-1}^2 + 1 \quad (4)$$

with $N_0 = 1$ and is bounded as follows [14]

$$2^{2^d} \leq N_{d+1} \leq 2^{\frac{5}{4} 2^d}. \quad (5)$$

The DWPT of a two-dimensional (2-D) image can be obtained by employing two separable 1D wavelet packets in each direction. The 4-ary nature of the wavelet packet tree now suggests

that the number of possible bases, N_d , satisfies the following equation

$$N_d = N_{d-1}^4 + 1 \quad (6)$$

with $N_0 = 1$ and is bounded as follows [17]

$$2^{4^d} \leq N_{d+1} \leq 2^{\frac{41}{40}4^d}. \quad (7)$$

This huge collection of wavelet packet bases must be searched to find an appropriate basis for a given image, resulting in a sparse representation adapted to the image contents with respect to certain criterion, as discussed below.

C. Basis Selection

It is clear from (7) that the number of possible bases N_d for a wavelet packet tree of depth d grows exponentially as d increases. A brute force approach that tries each possible basis to find out the most suitable one is, therefore, not practical. Coifman and Wickerhauser [6] applied Bellman's optimality principle (OP) to develop a fast algorithm which prunes the *full wavelet packet tree*² into the best wavelet packet tree for a given signal based on a particular cost function. According to the OP, an optimal subtree starting from a node λ_d^n at a depth d must include optimal subtrees starting from its child nodes λ_{d+1}^{2n} and λ_{d+1}^{2n+1} at depth $d+1$. In other words, the optimal subtrees of all the children nodes of a node should be known before deciding whether the children should be kept or merged. Let $\mathcal{C}(\mathbf{w}_\lambda)$ denote the cost of a subband node λ computed from wavelet packet coefficients $\mathbf{w}_\lambda \in \lambda$; for simplicity, we denote $\mathcal{C}(\mathbf{w}_\lambda)$ by $\mathcal{C}(\lambda)$. Starting from the terminal nodes of a full wavelet packet tree of depth J , the algorithm decides for each set of sibling nodes whether to keep them or their parent node λ_{j-1}^n , for all $0 \leq n < 2^{J-1}$ (see Figs. 1–4 for the convention used to denote these nodes in the case of images), depending on which of the following two is smaller: $\mathcal{C}(\lambda_j^{2n}) + \mathcal{C}(\lambda_j^{2n+1})$ or $\mathcal{C}(\lambda_{j-1}^n)$. Assuming that \mathcal{C} is an *additive* cost function³ a series of such decisions at depth $J-1$ to keep the children nodes (*split*) or to keep the parent node (*merge*) gives an optimal subtree for each node at depth $J-1$. Proceeding in a similar fashion in a bottom-up direction, the full wavelet packet tree can be pruned and the best basis with respect to \mathcal{C} can be obtained when we reach the root node λ_0^0 of the tree. The time complexity of this basis selection algorithm for a 1D signal is $O(N \log_2 N)$, where N denotes length of the signal. The extension of this algorithm to images is straightforward.

²A *full wavelet packet tree* is a wavelet packet tree whose each node except the leaf nodes has s children, where $s = 2^\nu$ and ν denotes the number of dimensions of the signal.

³A cost function $\mathcal{C}(\mathbf{w}_\lambda)$ of a vector \mathbf{w}_λ is called *additive* if it satisfies the following relation:

$$\mathcal{C}(\mathbf{w}_\lambda) = \mathcal{C}(\lambda) = \sum_{k=1}^{|\mathcal{P}|} \mathcal{C}(\mathbf{w}_{\lambda_k}),$$

where $|\mathcal{P}|$ denotes the number of partitions and \mathbf{w}_{λ_k} , $k = 1, 2, \dots, |\mathcal{P}|$, are nonoverlapping and completely covering partitions of \mathbf{w}_λ .

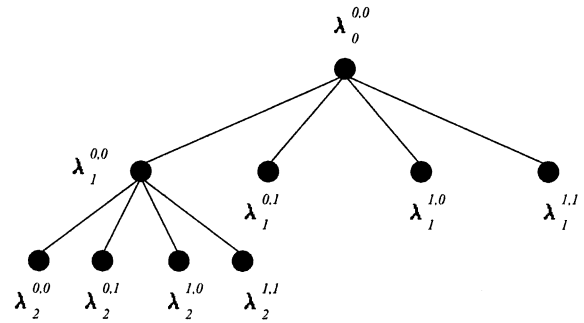


Fig. 1. Wavelet packet (WP) tree for a 2-level wavelet decomposition.

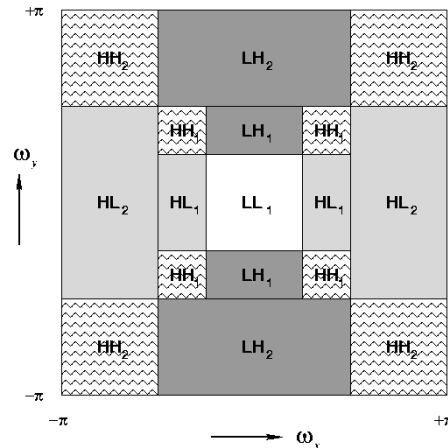


Fig. 2. Split of the 2-D spatial frequency plane due to a 2-level wavelet decomposition.

III. WAVELET PACKET ZEROTREES

Zerotree quantization is an effective way of exploiting the self-similarities among high frequency subbands at various resolutions. The main thrust of this quantization strategy is in the prediction of the significance of corresponding wavelet coefficients in higher frequency subbands at the finer resolutions by exploiting the parent-offspring relationship. This prediction works well, in terms of efficiently encoding the wavelet coefficients, due to the statistical characteristics of subbands at various resolutions and is related to the scale-invariance of edges in high frequency subbands of similar orientation. Moreover, embedded (progressive) transmission and reconstruction, which is required in some applications, using zerotrees with successive approximation quantization (SAQ), is quite straightforward.

In order to explore the possibility of wedding the wavelet packets with zerotrees, let us suppose first that the best basis has been selected and zerotree quantization is to be used to encode the wavelet packet transform coefficients. The issue is how to organize spatial orientation trees so as to exploit the self-similarities, if any, among the subbands. The wavelet packet subbands do not, apparently, yield parent-offspring relationships such as those present in the wavelet subbands. Let us try to extend the concept of zerotrees from the fixed wavelet scenario to the general wavelet packet case. Consider a square image of width $N = 2^{-L}$ belonging to the space V_{L^2} or $W_L^{0,0}$. A 2-level wavelet decomposition of this image can also be shown by a quadtree of depth 2, as in Fig. 1, each of whose interme-

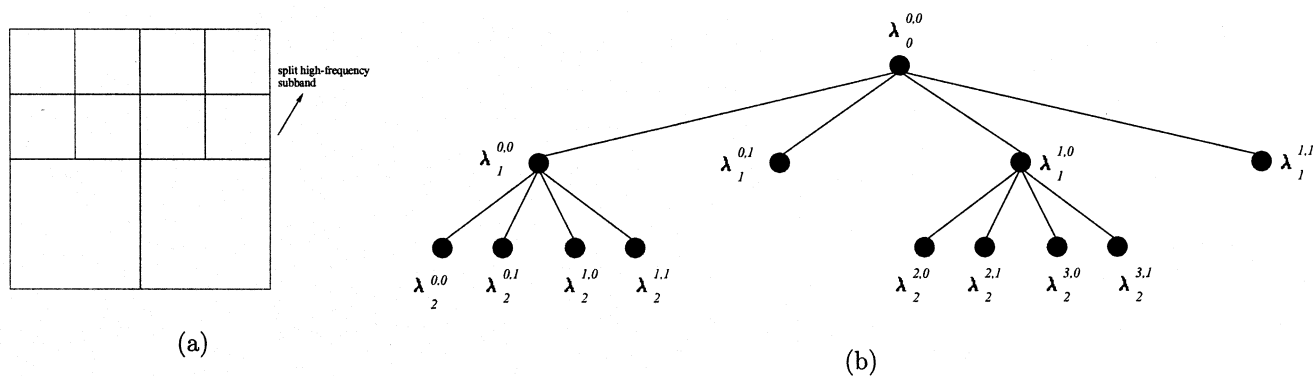


Fig. 3. WP tree for a simple 2-level WP decomposition.

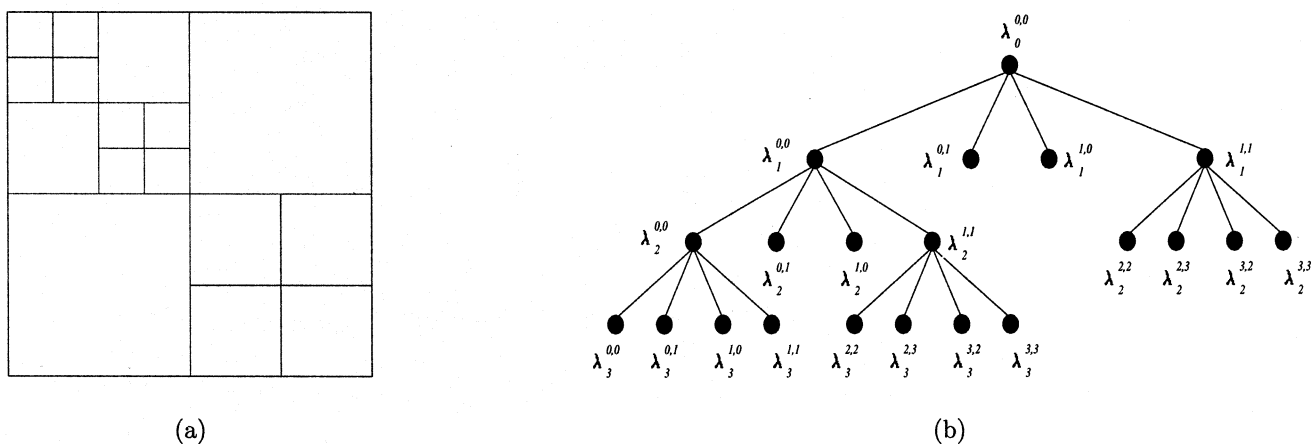


Fig. 4. WP tree for a 3-level WP decomposition.

diate nodes is associated with a corresponding subband and the root node $\lambda_0^{0,0}$ represents the original image. The node $\lambda_1^{0,1}$, for instance, corresponds to the subspace $W_{L+1}^{0,1}$ and the subband LH_1 , and so on. Each coefficient of $\lambda_2^{0,1}$ (LH_2) is associated with four coefficients belonging to $\lambda_1^{0,1}$ (LH_1) at corresponding spatial locations. In other words, it can be said that $\lambda_2^{0,1}$ is the parent node of $\lambda_1^{0,1}$ in the sense of zerotrees. A frequency split of all subbands in this decomposition, shown in Fig. 2, may be used in favor of this argument.

Now consider the 2-level wavelet packet decomposition and its corresponding tree shown in Fig. 3. Each coefficient of $\lambda_2^{1,0}$ can be spatially associated with four coefficients in $\lambda_2^{2,0}$, $\lambda_2^{2,1}$, $\lambda_2^{3,0}$, and $\lambda_2^{3,1}$. In other words, the node $\lambda_2^{1,0}$, which was the parent node of $\lambda_1^{1,0}$ in a wavelet tree, is the parent of all four children of $\lambda_1^{1,0}$ (the node with similar orientation, or same superscripts, at previous level). Consider now another 3-level wavelet packet decomposition and the corresponding tree shown in Fig. 4. This is just like a wavelet decomposition, except that the nodes $\lambda_2^{1,1}$ and $\lambda_1^{1,1}$ have been further split. The orientations of all children of $\lambda_2^{1,1}$ are the same as those of all of the children of $\lambda_1^{1,1}$. Therefore, each coefficient of $\lambda_3^{2,3}$, for instance, can be associated with four coefficients of $\lambda_2^{2,3}$ at a similar spatial location, due to their compatibility of orientation. This compatibility can be generalized to formulate a set of rules, presented in Section III-C, to construct the zerotree structure for an arbitrary wavelet packet geometry.

A. Compatible Zerotrees

Due to the dyadic nature of wavelet subbands, the organization of parent-child relationships is quite straightforward. If we look closely at the nature of the wavelet packet decomposition, we find that the subbands in a wavelet packet decomposition can be classified into three main categories, similar to three families of subbands in a wavelet decomposition. We call them *primary compatible zerotrees* to denote the trees of subbands having similar global orientation. The adjective *compatible* originates from the fact that these trees are generated taking into account both scale and orientation compatibility, as will be obvious from the rules for their construction. Let, \mathcal{H} , \mathcal{V} , and \mathcal{D} denote the families of subbands corresponding to the wavelet subbands (or their further decompositions) containing horizontal (LH), vertical (HL), and diagonal (HH) edges, respectively. The compatible zerotrees associated with the three families, \mathcal{H} , \mathcal{V} , and \mathcal{D} of a 3-level wavelet decomposition are shown in Fig. 5. It is to be noted that the compatible zerotrees differ from the zerotrees of [22] in the sense that the nodes of a compatible zerotree represent a full subband as opposed to an ordinary zerotree whose nodes represent one or more transform coefficients of a subband.

In the next section, we present a solution to the problem which occurs when a child node in the compatible zerotree is at a coarser resolution than the parent node, followed by a set of rules required to construct compatible zerotrees.

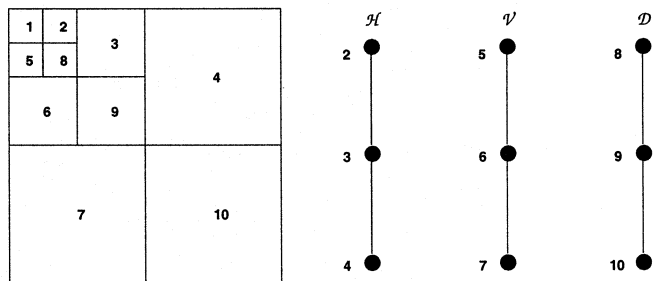


Fig. 5. Compatible zerotrees for the subband families \mathcal{H} , \mathcal{V} , and \mathcal{D} of a 3-level wavelet decomposition.

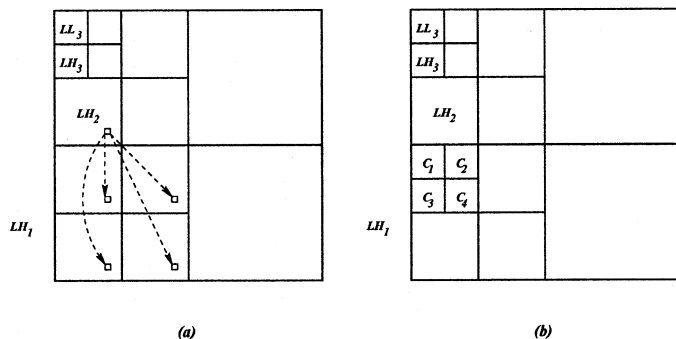


Fig. 6. Parenting conflict in a WP decomposition (a) WP subband decomposition with no parenting conflict (b) WP subband decomposition with parenting conflict arising from the split of one of the child nodes of the vertical high frequency subband LH_1 .

B. Parenting Conflict

As mentioned earlier, the high frequency subbands in a wavelet packet decomposition can be further decomposed in order to adapt the basis to the image contents. In a pre-decomposed tree of one of these families of subbands (\mathcal{H} , \mathcal{V} , and \mathcal{D}), if a child node is decomposed into only four subbands at the next coarser resolution, the parent-offspring relations are easy to establish, as shown in Fig. 6(a). However, if any of these four child nodes is decomposed any further, as shown in Fig. 6(b), the resulting subbands C_1, C_2, C_3 , and C_4 would be at a coarser resolution than the parent node (subband) LH_2 . This results in the association of each coefficient of such a child node to multiple parent coefficients, in the parent node, giving rise to a *parenting conflict*. In other words, there are four candidate coefficients in LH_2 claiming the parenthood of each of the four corresponding coefficients belonging to the child nodes C_i ($i = 1, \dots, 4$). One possible solution is to merge the four children so as to resolve the conflict [30]. This suboptimal approach constrains the basis selection process, resulting in a loss of freedom in adapting the wavelet packet basis to the contents of a given image. In order to resolve the parenting conflict, we suggest the following solution. Due to their orientation and scale compatibility with the subband LH_3 , these child nodes C_i ($i = 1, \dots, 4$) can be moved up in the tree so that they are linked directly to LH_3 , the root node of the primary compatible zerotree associated with the family \mathcal{V} of subbands. This should allow us to generate the compatible zerotree structure without restricting the basis selection.

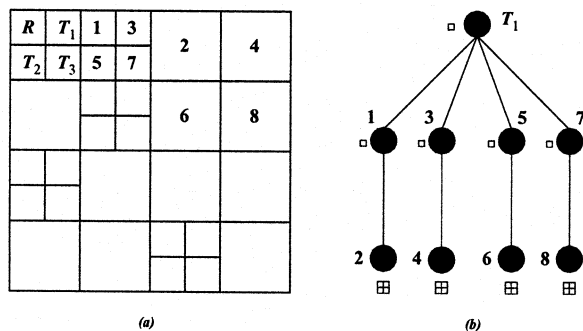


Fig. 7. A sample intermediate compatible zerotree (a) Sample geometry of a 3-level WP decomposition, and (b) the parent-offspring relationships for compatible zerotree originating from T_1 .

C. Rules for Generating the Compatible Zerotrees

In this section, we present a set of rules to construct the overall compatible zerotree structure for an arbitrary wavelet packet basis. The only assumption made is that the lowest frequency subband of the selected basis is always at the coarsest resolution. This is a reasonable assumption, based upon the fact that a significant amount of the signal energy is concentrated in the lowest frequency subband, which is most likely not to be merged by any of the tree pruning algorithms. In the description of these rules, “node X is followed by node Y ” refers to the situation where node X is at a higher level (or coarser resolution of pre-decomposed high frequency subbands, as in a wavelet decomposition) than the node Y in the hierarchy of subbands in a given family tree.

Rules

- If a node P at a coarser resolution is followed only by a node C at the next finer resolution (as in a wavelet transform), the node P is declared as a parent of C .
- If a node P is followed by four nodes C_1, C_2, C_3 , and C_4 (at the same resolution), then P is declared to be the parent of all these four nodes.
- If four subbands P_1, P_2, P_3 , and P_4 at a coarser resolution are followed by four subbands C_1, C_2, C_3 , and C_4 at the next finer resolution, then node P_i is declared to be the parent of node C_i (for $i = 1, 2, 3, 4$).
- If a node P is at a finer resolution than four of its children, say C_1, C_2, C_3 , and C_4 , then P is disregarded as being the parent of all these nodes and all of them are moved in the tree under a node at the same or a coarser resolution.

Consider the sample segmentation shown in Fig. 7(a). Let R denote the node representing the lowest frequency subband, situated in the top-left corner of a conventional subband decomposition. Then R represents the root node of an overall compatible zerotree with T_1, T_2 , and T_3 —which represent the coarsest resolution high frequency subbands—being its immediate children, as shown in Fig. 7(a). These child nodes are themselves roots of three compatible zerotrees corresponding to the families, \mathcal{H} , \mathcal{V} , and \mathcal{D} respectively. These compatible zerotrees are separately generated, only once for a given wavelet packet basis, in a recursive manner, using the rules described above. The construction of compatible zerotrees proceeds in two steps. In the

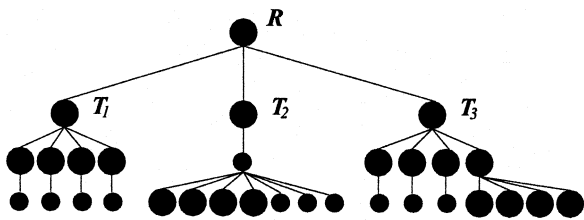


Fig. 8. The overall compatible zerotree structure comprising of the three primary compatible zerotrees T_1 , T_2 , and T_3 ; each node represents a whole WP subband, and the node radius corresponds to the support of basis functions at that transform level.

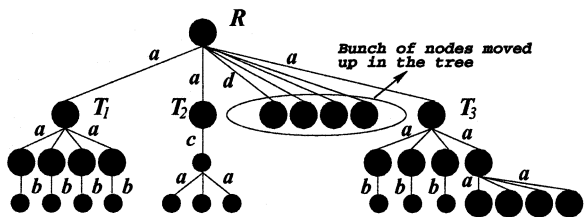


Fig. 9. The overall compatible zerotree structure, after re-organization to resolve the parenting conflicts; the edge labels depict the rules used to generate the links between parent and the child nodes.

first step, the primary compatible zerotrees corresponding to the subband families, \mathcal{H} , \mathcal{V} , and \mathcal{D} , and are constructed using rules a , b , and c . In the second step, the overall tree is reorganized using rule d , in order to resolve any parenting conflicts. Let us consider the segmentation shown in Fig. 7(a) to explain these rules. The primary compatible zerotrees T_1 , T_2 , and T_3 are generated, as shown in Fig. 8, in the first step. The overall tree is re-organized (as shown in Fig. 9) using rule d in order to resolve the parenting conflict under node P . This rule first identifies nodes with the parenting conflicts and when such nodes are found, the whole bunch (consisting of C_1 , C_2 , C_3 , and C_4) is plucked from its current position in the tree. The algorithm then climbs up the tree to look for an appropriate node, a compatible ancestor at the nearest scale and having the nearest orientation, and glues the bunch under this newly found compatible parent. The parent-offspring dependences for the primary compatible zerotree T_1 are shown in Fig. 7(b).

In the case of zerotrees for wavelet subbands, where each parent subband node is followed by exactly one child subband of similar orientation at the next finer resolution and thus each coefficient of the parent node is associated with four coefficients of the child node at some spatial location, an intermediate node in a compatible zerotree, in general, can have more than one child node. In a compatible zerotree, the parent-offspring relationships are established by looking at the scale of subband nodes in the tree. What determines the parent-offspring relationships between their coefficients is the difference in scale of the parent and child nodes. For instance, if both parent and the child nodes are at the same scale, each coefficient of the parent node will have exactly one offspring coefficient at same spatial location in the child node, whereas if the parent node is at the immediate coarser resolution than the child node, then each coefficient of the parent node is associated with four coefficients at the same spatial location in the child node.

IV. COMPATIBLE ZEROTREE HYPOTHESIS

Given an arbitrarily segmented wavelet packet basis, compatible zerotrees are constructed using the algorithm described above. In order to be able to make predictions for wavelet packet coefficients in finer resolution subbands, the *compatible zerotree hypothesis* is defined as follows. *If a wavelet packet coefficient of a node from the compatible zerotree is insignificant, it is more likely that the wavelet packet coefficients at similar spatial locations in all the descendant nodes of the same compatible zerotree will be insignificant as well.* Compatible zerotrees provide us a convenient way of making predictions about the insignificance of corresponding coefficients in the child nodes, given the significance of a coefficient belonging to the parent node.

The success of the compatible zerotree hypothesis for wavelet packets, as defined above, can be tested by employing two empirical approaches. First, the amplitude of transform coefficients is plotted for all the subbands organized both in the ordinary increasing frequency order and in the compatible zerotrees. Consider the plots of wavelet coefficient amplitude against the coefficient indices for a 5-level wavelet decomposition of the 512×512 *Barbara* image, as shown in Fig. 11. The amplitude axis in both plots was restricted to ± 1000 to facilitate the display of smaller coefficients. While the subbands were arranged in an increasing frequency order for the plot in Fig. 11(a), the plot in Fig. 11(b) refers to the subbands as organized in the compatible zerotrees. Similar plots of wavelet packet coefficients' amplitudes against the coefficient indices for the same image using the basis geometry⁴ shown in Fig. 10(a) are provided in Fig. 12. In all plots corresponding to the subbands organized in the compatible zerotrees, three families of primary compatible zerotrees T_1 , T_2 , and T_3 are clearly visible, showing that the new arrangement is successful in isolating the coefficients of similar orientation in a hierarchy to be used for prediction in a top-down fashion. Zoomed plots of these families, as shown in Fig. 13, exhibit more sub-families organized within these compatible zerotrees.

An alternate approach to test the success of compatible zerotree hypothesis is to compute the conditional probability $p(x|y)$ of the significance of a child coefficient x given the significance of its parent coefficient y for a specific threshold value. We plotted both joint and the conditional histograms to verify how successfully the prediction for insignificance of a coefficient in a child subband can be made given the significance of its parent coefficient. The joint and conditional histograms for some parent subbands and their immediate children using the subband decomposition of Fig. 10(a) for *Barbara* are shown in Fig. 14 and Fig. 15. These histograms were obtained by accumulating the joint and conditional significance probability counts after a uniform scalar quantization of the subbands, where the values on x and y axes represent the quantization index. In these histograms, a value for probability count is represented by a gray level, with white representing high probability count and black representing low probability

⁴The corresponding compatible zerotrees are shown in the Fig. 10(b) with a numbering generated in a recursive manner.

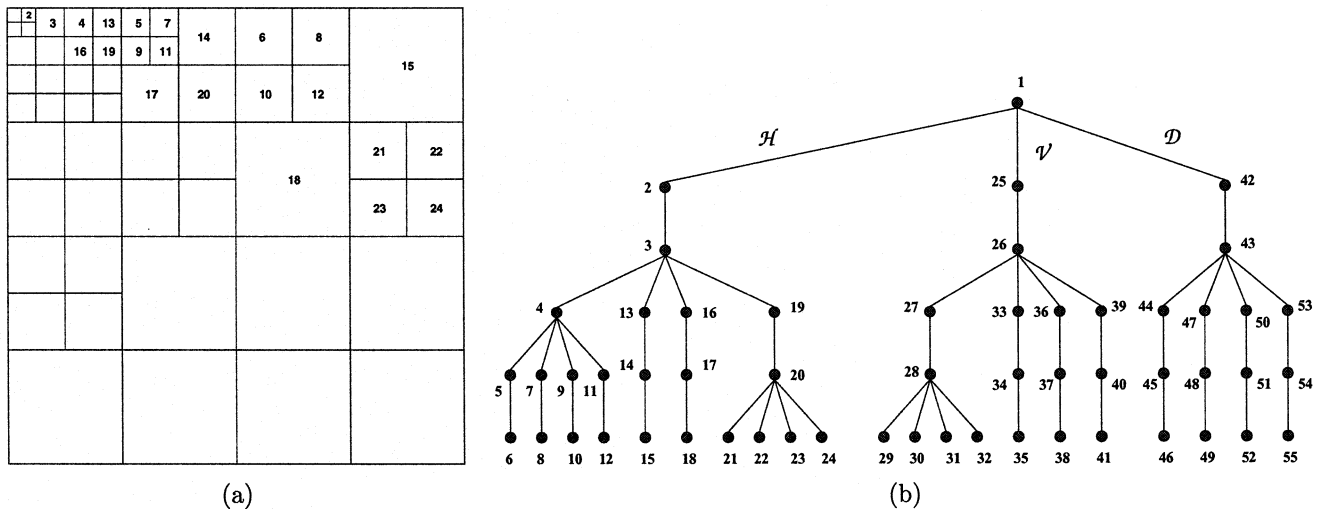


Fig. 10. A sample WP geometry and corresponding compatible zerotrees (a) WP decomposition used for illustration of the compatible zerotree hypothesis for WP's, and (b) Compatible trees for the decomposition in (a); Nodes are labeled in a recursive fashion, as shown in part (b).

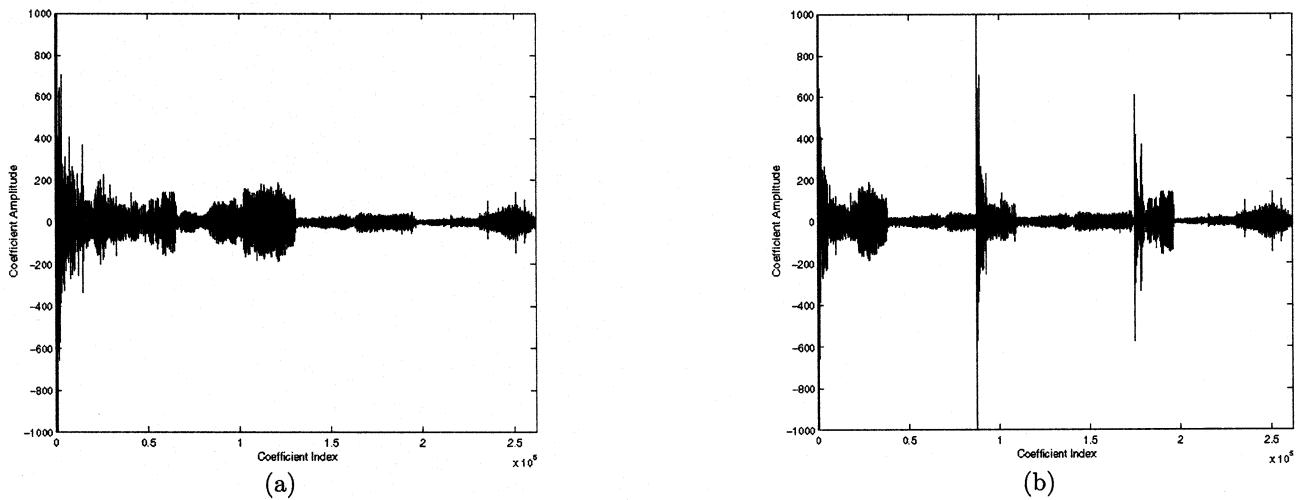


Fig. 11. Plot of wavelet coefficients' amplitude vs. coefficient indices for 5-level wavelet decomposition of *Barbara*. The subbands were arranged in (a) an increasing frequency order, and (b) a compatible zerotree order.

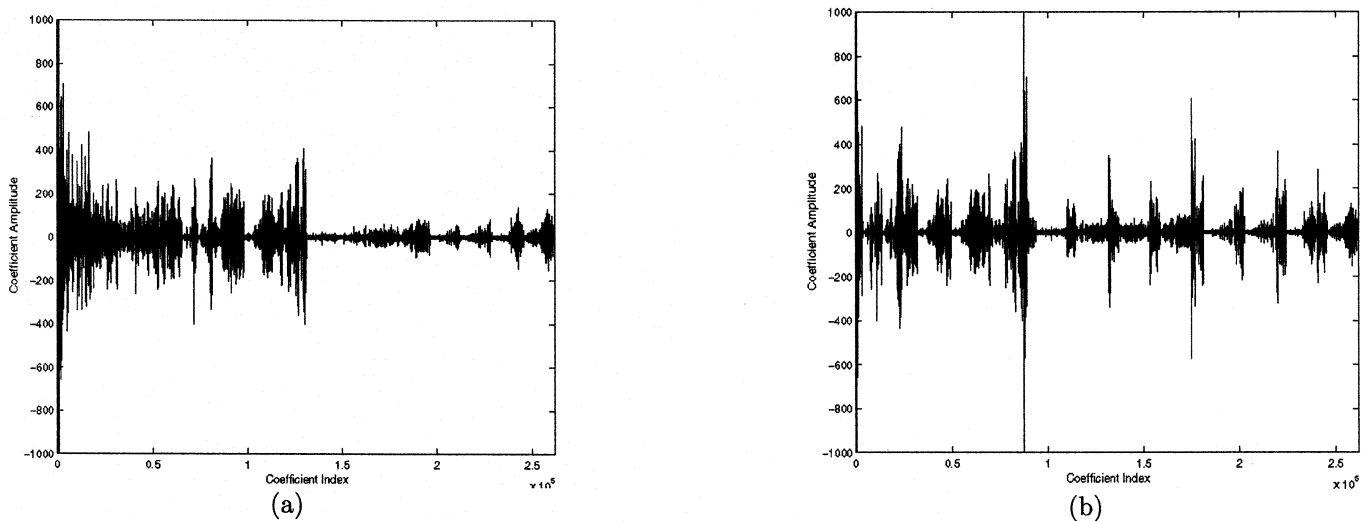


Fig. 12. Plot of WP coefficients' amplitude vs. coefficient indices for WP decomposition shown in Fig. 10(a) of *Barbara*. The subbands were organized in (a) an increasing frequency order, and (b) a compatible zerotree order.

count. The concentration of these histograms in the low significance range of child coefficients throughout the range of parent

coefficients is encouraging evidence for the organization of these subbands in a compatible zerotree order.

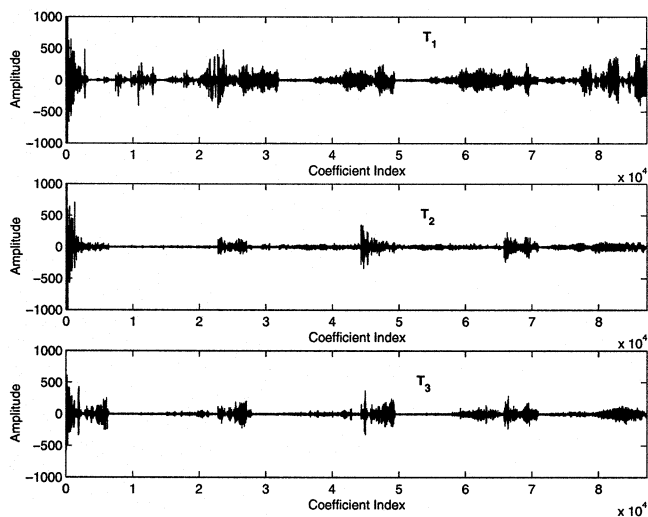


Fig. 13. Zoomed sections of Fig. 12(b) the families T_1 , T_2 , and T_3 showing more sub-families within these compatible zerotrees.

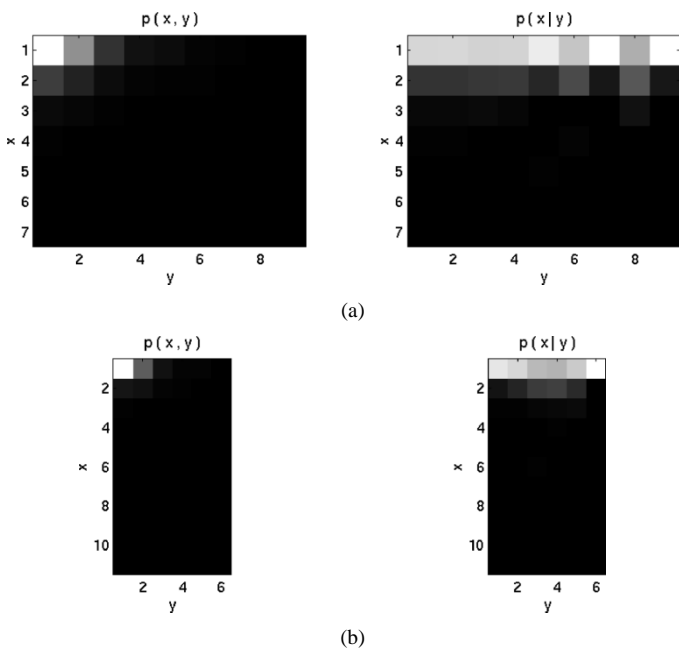


Fig. 14. Joint and conditional histograms for subbands numbered 3 and 4 (a) subband 3 and its immediate children; $\text{binsize} = 80$, and (b) subband 4 and its immediate children; $\text{binsize} = 50$.

V. MARKOV CHAIN BASED COST ESTIMATION

Coifman and Wickerhauser [6] suggested using an *entropy*-based cost function in order to select the best basis resulting in compaction of the overall energy. This cost function, however, does not take into account the quantization strategy employed by the coder. Moreover, using this cost function does not necessarily yield a meaningful basis [15]. In order to ensure that the selected basis is *zerotree friendly*, we propose using a cost function that can estimate the entropy of quantized coefficients belonging to the compatible zerotrees.

If the compatible zerotree hypothesis is true, the insignificance of child coefficients in a subband is related to the insignificance of their parent coefficient. This would suggest that the subbands (nodes) belonging to each family of the compatible

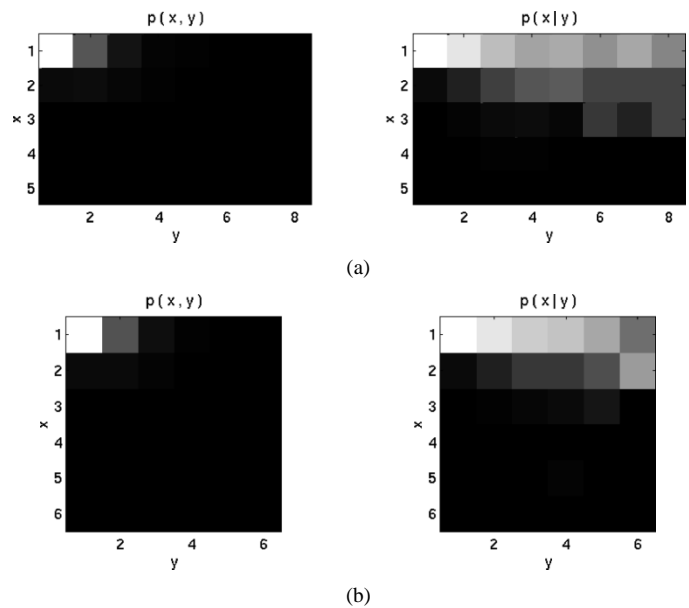


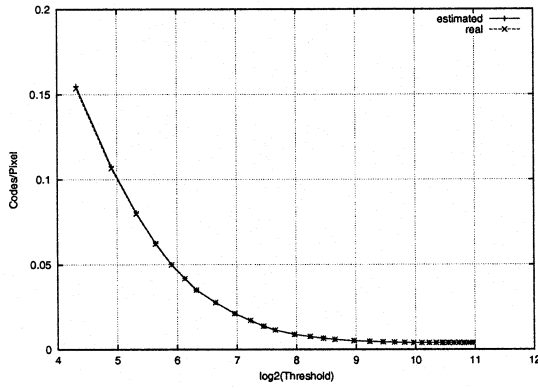
Fig. 15. Joint and conditional histograms for subbands numbered 26 and 43 (a) subband 26 and its immediate children; $\text{binsize} = 100$, and (b) subband 43 and its immediate children; $\text{binsize} = 80$.

zerotrees can be modeled as a nonhomogeneous Markov chain (MC) with time replaced by node depth in the tree, i.e., the root compatible zerotree. Let X_j denote a random variable corresponding to the significance of coefficients of all nodes at depth j of the compatible zerotree that are the children of coefficients belonging to the corresponding parent node at tree depth $j - 1$. The sample space S for these random variables X_1, X_2, \dots, X_J (where J denotes depth of the tree or the number of transform levels) is $S = \{0, 1, \zeta\}$, where a value of 0 denotes that the coefficient is insignificant with respect to a threshold, a value of 1 denotes its magnitude being larger than the threshold, and a value of ζ denotes that the coefficient will be encoded as a zerotree symbol.

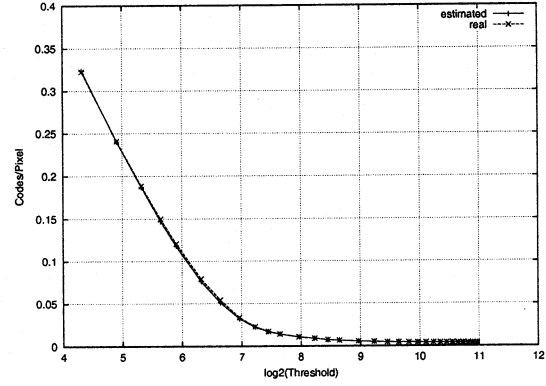
The performance of zerotree encoding depends largely upon the values of mutual information $I(X_j, X_{j+1})$, where $0 \leq j < J$, for a given basis. The larger the sum of these values, the more efficient the encoding is. Given a basis \mathcal{B} for an image, this value determines how *friendly* the basis \mathcal{B} would be to the zerotree quantization method. The cost $C_{zt}(\mathbf{w}, \mathcal{B})$ of encoding the coefficients \mathbf{w} of a J -level wavelet packet basis \mathcal{B} can be written as

$$C_{zt}(\mathbf{w}, \mathcal{B}) = \sum_{l=0}^{N_l-1} [C_{sm}(\mathbf{w}, T_l) + C_{re}(\mathbf{w}, T_l)] \quad (8)$$

where $T_l = T_0/2^l$ is the threshold value used at the l th iteration, $T_0 = \max(|w_k|)$, N_l denotes the number of iterations of encoding, and C_{sm} and C_{re} denote the costs of encoding the significance map (ie, information about significance of each of the coefficients with respect to the threshold T_l) and the refinement information (required to successively update magnitude of the coefficient) respectively. It was our observation that the symbol used to encode the refinement information using zerotree quantization was nearly random. This led to the conclusion that it would suffice to approximate $C_{zt}(\mathbf{w}, \mathcal{B})$ by estimating only the



(a)



(b)

Fig. 16. Cost of encoding the significance map vs. threshold value: (a) Lena and (b) Barbara.

1. Compute the J -level full wavelet packet tree decomposition.
 2. Initialize $j \leftarrow J - 1$.
 3. For all $0 \leq p < 2^j, 0 \leq q < 2^j$, do the following:
 - a) Compute $\mathcal{C}(f, \mathcal{B}_j^{p,q})$ and $\mathcal{C}(f, \mathcal{B}_{j+1}^{p,q})$ using equations (10) and (11).
 - b) If $\mathcal{C}(f, \mathcal{B}_j^{p,q}) > \mathcal{C}(f, \mathcal{B}_{j+1}^{p,q})$,
 - keep the four child subbands at depth $j + 1$,
 - otherwise
 - merge them to get $\lambda_j^{p,q}$.
 4. Decrement j by 1.
 5. If $j < 0$, then stop, otherwise go to step 3.
- Fig. 17. Best basis selection algorithm for zerotree quantization.

TABLE I
CZQ COMPRESSION RESULTS FOR 512×512 LENA IMAGE

Bit rate (bpp)	Compression ratio (:1)	PSNR (dB)		
		SPIHT	CZQ-WV	CZQ-WP
1.0	8	40.41	40.06	40.10
0.8	10	39.32	38.74	38.85
0.7	11.43	38.73	38.35	38.47
0.6	13.33	38.01	37.96	38.08
0.5	16	37.21	37.50	37.55
0.4	20	36.23	35.86	36.02
0.3	26.67	34.94	34.89	35.06
0.25	32	34.11	34.49	34.56
0.2	40	33.15	32.89	32.90
0.1	80	30.23	29.90	29.95

first term in above expression. The cost C_{sm} can be estimated by computing the entropy of a discrete random variable whose

TABLE II
CZQ COMPRESSION RESULTS FOR 512×512 GOLDHILL IMAGE

Bit rate (bpp)	Compression ratio (:1)	PSNR (dB)		
		SPIHT	CZQ-WV	CZQ-WP
1.0	8	36.55	34.84	35.01
0.8	10	35.91	34.16	34.30
0.7	11.43	34.63	33.81	33.91
0.6	13.33	33.93	32.63	32.83
0.5	16	33.13	31.69	31.94
0.4	20	32.18	31.02	31.25
0.3	26.67	31.15	30.36	30.54
0.25	32	30.56	29.75	29.88
0.2	40	29.85	28.81	28.98
0.1	80	27.93	27.35	27.48

value is drawn from the set of codewords used to encode the significance map. These codewords include two symbols (0 and 1) to represent whether a coefficient is significant or not, and a zerotree symbol whose probability can be computed as follows.

Let $P_k(0)$ denote $Pr(X_k = 0)$, the probability of a coefficient belonging to subband nodes at tree depth k being insignificant, and $P_{j,i}(0|0)$ denote the probability of all child coefficients at depth j to be insignificant given that all of their corresponding parent coefficients at the previous depth i are insignificant. Let $P_k(\zeta)$ denote the joint probability of all the coefficients originating from nodes at tree depth k and all their child coefficients being insignificant. In other words, it denotes the probability of a zerotree of length $J-k$, which consists of $(4^{J-k+1} - 1)$ coefficients in a wavelet zerotree. According to the multidimensional probability mass function (pmf) theorem of Markov chains [25], $P_k(\zeta)$ is given by

$$P_k(\zeta) = P_k(0)P_{k+1,k}(0|0)P_{k+2,k+1}(0|0) \cdots P_{J,J-1}(0|0) \quad (9)$$

TABLE III
 CZQ COMPRESSION RESULTS FOR 512×512 *BARBARA* IMAGE

Bit rate (bpp)	Compression ratio (:1)	PSNR (dB)		
		SPIHT	CZQ-WV	CZQ-WP
1.0	8	36.41	35.14	36.15
0.8	10	34.66	32.64	33.91
0.7	11.43	33.75	32.04	33.21
0.6	13.33	32.53	31.50	32.56
0.5	16	31.40	30.28	31.60
0.4	20	30.10	28.41	29.85
0.3	26.67	28.56	27.50	28.77
0.25	32	27.58	27.12	28.12
0.2	40	26.65	25.25	26.64
0.1	80	24.26	23.64	24.27

 TABLE IV
 CZQ COMPRESSION RESULTS FOR 512×512 *FINGERPRINTS* IMAGE

Bit rate (bpp)	Compression ratio (:1)	PSNR (dB)		
		SPIHT	CZQ-WV	CZQ-WP
1.0	8	36.02	35.24	35.82
0.8	10	34.29	32.71	33.38
0.7	11.43	33.38	31.84	32.45
0.6	13.33	32.37	31.12	31.74
0.5	16	31.27	30.65	31.15
0.4	20	29.92	28.39	29.09
0.3	26.67	28.25	27.00	27.64
0.25	32	27.12	26.53	27.07
0.2	40	26.01	25.08	25.64
0.1	80	23.23	22.84	23.24



(a)



(b)

 Fig. 18. Two original 512×512 test images (a) *Barbara* and (b) *Fingerprints*.

or

$$P_k(\zeta) = P_k(0) \prod_{j=k}^{J-1} P_{j+1,j}(0|0). \quad (10)$$

The cost C_{sm} can now be computed as follows:

$$C_{sm} = - \sum_{k=1}^J \sum_{s \in S} P_k(s) \log P_k(s). \quad (11)$$

The above equation provides us a way of estimating the cost of using a particular basis for encoding wavelet packet transformed images with compatible zerotree quantization. The most cost effective (*best*) basis for this particular quantizer can be obtained

by minimizing (8). Fig. 16 shows the graph of the cost of encoding the significance map (both estimated and real) in terms of the number of codewords per pixel plotted against various threshold values for both *Lena* and *Barbara* images. It is assumed that given a coefficient and all its child coefficients are insignificant, it is very likely that its siblings and all their children are insignificant too. The probability $P_{j,j-1}(0|0)$ can, therefore, be approximated by the probability of all four child coefficients at depth j being insignificant given that their parent coefficient at depth $j - 1$ is insignificant. From these graphs, it is clear that this estimation works better for the *Lena* image than for the *Barbara* image, due to the latter's being of a relatively complex nature. The MC based computation of the cost of encoding the

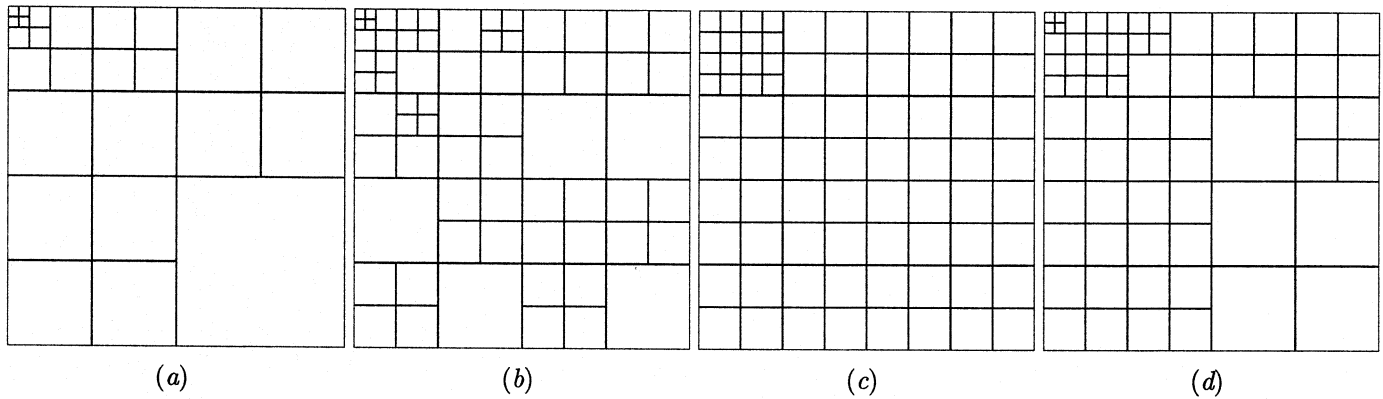


Fig. 19. Selected 2-D WP bases used for encoding (a) *Lena*, (b) *Goldhill*, (c) *Barbara*, and (d) *Fingerprints*.

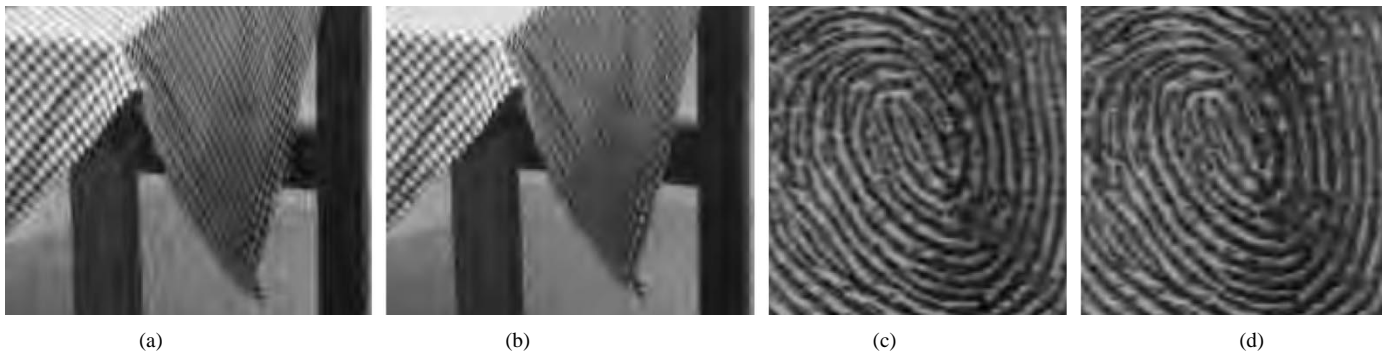


Fig. 20. Visual quality of coding results Portion of *Barbara* (table cloth) encoded at 0.25 bpp (a) CZQ- \mathcal{WP} and (b) SPIHT; Portion of *Fingerprints* (central spiral) encoded at 0.25 bpp (c) CZQ- \mathcal{WP} and (d) SPIHT.

significance map proves to be a good estimate, particularly at large threshold values which correspond to low bit rates.

VI. CODING ALGORITHM AND RESULTS

A. Basis Selection Algorithm

As discussed earlier in the previous section, the use of a bottom-up search method, along with a cost function that takes into account the quantization strategy, ensures selection of the best basis for compressing a given image using that particular quantization method. Based on the cost estimate described in the previous section, a bottom-up basis selection algorithm can be used to select what can be termed as a *zerotree friendly* wavelet packet basis. Let the given image I be of size $N \times N$. Let $\lambda_j^{p,q}$ denote a node in the wavelet packet tree corresponding to a subband at depth j and $\lambda_{j+1}^{2p,2q}$, $\lambda_{j+1}^{2p+1,2q}$, $\lambda_{j+1}^{2p,2q+1}$, and $\lambda_{j+1}^{2p+1,2q+1}$ be the four child nodes at depth $j+1$ corresponding to the decomposition of $\lambda_j^{p,q}$. There are up to 4^j subband nodes at each depth j associated with $0 \leq p < 2^j$ and $0 \leq q < 2^j$. The algorithm for selection of the best basis using the new paradigm and the cost estimate for $\mathcal{C}(f, \mathcal{B})$ is given in Fig. 17. This algorithm takes $O(N \log_2 N)$ time to select the best wavelet packet basis for compatible zerotree quantization. However, when comparing it to the Coifman-Wickerhauser algorithm for basis selection, it should be noted that the cost $\mathcal{C}(f, \mathcal{B})$ is calculated by taking into account all the current terminal nodes instead of only the nodes in question (ie, the parent node $\lambda_j^{p,q}$ at depth j and its four child nodes at depth $j+1$). This is due to the nature of quantization method we

are considering and does not necessarily need to be the case if another quantization method is used.

B. Experimental Results and Discussion

Given a basis, the compatible zerotrees can be organized using the rules given in [18]. Once the compatible zerotrees have been generated, based upon knowledge of the best basis, the coding is performed by successively encoding the significance information about the coefficients, as they appear in the subbands in an increasing frequency order, and the refinement information until the bit budget has expired or the encoded bitstream terminates, whichever happens earlier. This makes the decoder capable of generating an approximation to the original image at any given bit rate or quality, as long as the minimum required bits are available for doing so.

Experiments were conducted on four standard 8-bit greyscale images of resolution 512×512 —*Lena*, *Goldhill*, *Barbara*, and *Fingerprints*—using both a wavelet basis and a zerotree friendly wavelet packet basis selected by the algorithm mentioned above. For all the experiments, the factorized 9–7 biorthogonal filters [15] were used for efficiently computing the wavelet packet transform. Results for the performance of both variants of the compatible zerotree quantization (CZQ) coder—first using the wavelet basis CZQ- \mathcal{WV} and other using the zerotree friendly wavelet packet basis CZQ- \mathcal{WP} —for all the test images are presented in Tables I–IV. The measure used to describe the performance of each coder is the peak-signal-to-noise-ratio (PSNR) defined as $10 \log_{10}[255^2/MSE]$, where MSE denotes the mean squared error, versus the bit-rate given in terms of bits per pixel

(bpp). Although it is well known that PSNR is not a representative measure of the performance from a perceptual viewpoint [10], it is still widely used for comparing the coding performances in quantitative terms. Like SPIHT and many other image coding algorithms, our algorithm also requires the full image and its wavelet packet transform to be held in memory.

While being capable of progressively reconstructing the encoded image and being relatively faster than other wavelet packet coders (such as [15] and [30]), the CZQ- \mathcal{WP} coder performs comparably well. The coding gains achieved by it on top of CZQ- \mathcal{WV} (nearly 0.1 dB for *Lena*, 0.1–0.25 dB for *Goldhill*, 0.6–1.5 dB for *Barbara*, and 0.4–0.7 dB for *Fingerprints*) empirically demonstrate success of the compatible zerotree hypothesis. We note that the superior coding performance of SPIHT as compared to CZQ- \mathcal{WV} is due to the fact that CZQ- \mathcal{WV} is just a variation of the EZW algorithm and does not employ the set partitioning rules of SPIHT. A closer look, however, at the reconstructed images by CZQ- \mathcal{WP} and SPIHT at 0.25 bpp reveals that CZQ- \mathcal{WP} yields better visual quality than SPIHT. Note, for instance, the quality of a portion (table cloth) of the reconstructed *Barbara* image encoded by CZQ- \mathcal{WP} and SPIHT, and the quality of a portion (central spiral) of the reconstructed *Fingerprints* image encoded by CZQ- \mathcal{WP} and SPIHT as shown in Fig. 20 (the original images are shown in Fig. 18). Fig. 19 shows the geometries of the 2-D wavelet packet bases selected for all test images. As expected, the basis selected for *Lena* closely resembles a wavelet basis, due to its being a smooth image.

VII. CONCLUSIONS

We have presented a general zerotree structure for adaptive wavelet transform that allows us to efficiently encode the transform coefficients and to progressively encode the image. The best basis was selected using a cost function that estimates the cost of zerotree quantization, in order to ensure that the resulting basis will be adapted to the image contents and the purpose of representation. Although experimental results show that the performance of our wavelet packet zerotree CZQ- \mathcal{WP} coder, in terms of both PSNR and visual quality, is significantly better than its wavelet counterpart CZQ- \mathcal{WV} , it is only marginally comparable to other wavelet packet coders such as [15], [30]. A possible explanation for this is the relative simplicity of our coder as compared to [30] and its inability to exploit intra-subband redundancies, as is the case in [15]. However, our coder maintains the better visual quality performance of wavelet packet image coders for complex textured images, such as *Barbara* and *Fingerprints*, over the wavelet based SPIHT image coder at low bit rates.

REFERENCES

- [1] P. J. Burt and E. H. Adelson, "The Laplacian pyramid as a compact image code," *IEEE Trans. Commun.*, vol. 31, pp. 532–540, 1983.
- [2] H. D. Cho and J. B. Ra, "A rearrangement algorithm of wavelet packet coefficients for zerotree coding," in *IEEE Int. Conf. Image Processing*, vol. 3, Oct. 1999, pp. 556–559.
- [3] R. J. Clarke, *Transform Coding of Images*. New York: Academic, 1985.
- [4] R. R. Coifman and Y. Meyer, "Orthonormal Wave Packet Bases," Dept. Math., Yale Univ., New Haven, CT, 1990.

- [5] —, "Size properties of wavelet packets" (in Russian), in *Wavelets and Their Applications*. New York: Jones and Bartlett, 1992, pp. 125–150.
- [6] R. R. Coifman and M. V. Wickerhauser, "Entropy-based algorithms for best basis selection," *IEEE Trans. Inform. Theory*, vol. 38, pp. 713–718, Mar. 1992.
- [7] I. Daubechies, "Orthonormal bases of compactly supported wavelets," *Commun. Pure Appl. Math.*, vol. 41, pp. 909–996, 1988.
- [8] D. L. Donoho, M. Vetterli, R. A. Devore, and I. Daubechies, "Data compression and harmonic analysis," *IEEE Trans. Inform. Theory*, vol. 44, pp. 2435–2476, 1998.
- [9] A. Grossman and J. Morlet, "Decomposition of Hardy function into square integrable wavelets of constant shape," *SIAM J. Appl. Math.*, pp. 723–773, June 1984.
- [10] N. J. Jayant, J. Johnstone, and B. Safranek, "Signal compression based on models of human perception," *Proc. IEEE*, vol. 81, pp. 1385–1422, Oct. 1993.
- [11] J. J. Koenderink, "Operational significance of receptive field assemblies," *Biol. Cybern.*, vol. 58, pp. 163–171, 1988.
- [12] S. Mallat, "A compact multiresolution representation: the wavelet model," in *Proc. IEEE Comput. Soc. Workshop Computer Vision*, 1987, pp. 2–7.
- [13] —, "A theory for multiresolution signal decomposition," *IEEE Trans. Pattern Anal. Machine Intell.*, vol. 11, pp. 674–693, 1989.
- [14] —, *A Wavelet Tour of Signal Processing*. New York: Academic, 1998.
- [15] F. G. Meyer, A. Z. Averbuch, and J.-O. Strömberg, "Fast adaptive wavelet packet image compression," *IEEE Trans. Image Processing*, vol. 9, pp. 792–800, May 2000.
- [16] Y. Meyer, "Principe d'incertitude, bases Hilbertiennes et algèbres d'opérateurs," *Sem. Bourbaki*, vol. 662, 1985.
- [17] N. M. Rajpoot, "Adaptive Wavelet Image Compression," Ph.D. dissertation, Dept. Computer Science, Univ. Warwick, Coventry, U.K., Apr. 2001.
- [18] N. M. Rajpoot, F. G. Meyer, R. G. Wilson, and R. R. Coifman, "Wavelet Packet Image Coding Using Compatible Zerotree Quantization," Dept. Comput. Sci., Yale Univ., New Haven, CT, YALEU/DCS/RR-1187, Sept. 1999.
- [19] K. Ramchandran and M. Vetterli, "Best wavelet packet bases in a rate-distortion sense," *IEEE Trans. Image Processing*, pp. 160–175, Apr. 1993.
- [20] A. Rosenfeld and M. Thurston, "Edge and curve detection for visual scene analysis," *IEEE Trans. Comput.*, vol. 20, pp. 562–569, 1971.
- [21] A. Said and W. A. Pearlman, "A new fast and efficient image codec based on set partitioning in hierarchical trees," *IEEE Trans. Circuits Syst. Video Technol.*, vol. 6, pp. 243–250, June 1996.
- [22] J. M. Shapiro, "Embedded image coding using zerotrees of wavelet coefficients," *IEEE Trans. Signal Processing*, pp. 3445–3462, Dec. 1993.
- [23] J.-O. Strömberg *et al.*, "A modified Franklin system and higher order spline systems on \mathbb{R}^n as unconditional bases for Hardy spaces," in *Proc. Conf. Honor of A. Zygmund*, Wadsworth Mathematical Series, W. Beckner *et al.*, Eds., 1981, pp. 475–493.
- [24] S. L. Tanimoto and T. Pavlidis, "A hierarchical data structure for picture processing," *Comput. Graph. Image Process.*, vol. 4, pp. 104–119, 1974.
- [25] Y. Viniotis, *Probability and Random Processes for Electrical Engineers*. New York: McGraw-Hill, 1998.
- [26] R. Wilson and M. Spann, *Image Segmentation and Uncertainty*. New York: Wiley, 1988.
- [27] A. P. Witkin, "Scale space filtering," in *Proc. IJCAI*, Karlsruhe, Germany, 1983.
- [28] J. W. Woods, *Subband Image Coding*. Norwell, MA: Kluwer, 1991.
- [29] Z. Xiong, K. Ramchandran, and M. T. Orchard, "Space-frequency quantization for wavelet image coding," *IEEE Transactions on Image Processing*, vol. 6, no. 5, pp. 677–693, 1997.
- [30] —, "Wavelet packet image coding using space-frequency quantization," *IEEE Trans. Image Processing*, vol. 7, no. 6, pp. 892–898, 1998.



Nasir M. Rajpoot (M'01) received the B.Sc. in mathematics and physics and M.Sc. in computer science, both with the highest distinctions, from Bahauddin Zakariya University, Pakistan, in 1991 and 1994 respectively. During 1994–1996, he studied on a Fellowship for his M.Sc. in systems engineering at Quaid-e-Azam University, Islamabad, Pakistan. In 2001, he received the Ph.D. from the Department of Computer Science, University of Warwick, Coventry, U.K., where he is currently a Lecturer.

His research interests are image and video coding, texture analysis, high-dimensional data analysis, and data compression.



Roland G. Wilson received the B.Sc. and Ph.D. degrees from the Department of Electrical and Electronic Engineering at the University of Glasgow, Glasgow, U.K., in 1971 and 1978, respectively.

From 1978 to 1985, he was a Lecturer in the Department of Electronic and Electrical Engineering at the University of Aston. In 1982–1983, he was a Visiting Professor at Linköping University, Linköping, Sweden. In 1985, he was appointed to a Senior Lectureship in the Department of Computer Science at the University of Warwick, Coventry, U.K. In 1992,

he was promoted to a Readership. In 1999, he was promoted to a Professorship. He has published over 100 papers in the areas of communication theory, image and audio signal processing and neural networks. He is an editorial board member for the journal *Pattern Recognition*.

Dr. Wilson was jointly awarded the Pattern Recognition Society Medal for Best Paper in Pattern Recognition with his student M. Spann in 1985.



François G. Meyer (M'94) graduated with Honors from Ecole Nationale Supérieure d'Informatique et de Mathématiques Appliquées, Grenoble, in 1987, with a M.S. in computer science and applied mathematics. He received a Ph.D. degree in electrical engineering from INRIA, France, in 1993.

From 1993 to 1995, he was a Postdoctoral Associate in the Departments of Diagnostic Radiology and Mathematics, Yale University, New Haven, CT. From 1996 to 1999, he was a faculty member of the Departments of Radiology, and Computer Science,

Yale University. He is currently an Assistant Professor with the Department of Electrical Engineering, University of Colorado, Boulder. His research interests include image and signal processing. He is the editor (with A. Petrosian) of *Wavelets in Signal and Image Analysis, From Theory to Practice* (Norwell, MA: Kluwer, 2001).



Ronald R. Coifman received the Ph.D. degree from the University of Geneva, Geneva, Switzerland, in 1965.

He is Phillips Professor of mathematics at Yale University, New Haven, CT. He was a Professor at Washington University, St. Louis, MO. His recent publications have been in the areas of nonlinear Fourier analysis, wavelet theory, numerical analysis, and scattering theory. He is currently leading a research program to develop new mathematical tools for efficient transcription of physical data, with

applications to feature extraction, recognition and denoising. He was chairman of the Yale Mathematics Department from 1986 to 1989.

Dr. Coifman is a member of the National Academy of Sciences, American Academy of Arts and Sciences, and the Connecticut Academy of Sciences and Engineering. He received the DARPA Sustained Excellence Award in 1996, the 1996 Connecticut Science Medal, the 1999 Pioneer award from the International Society for Industrial and Applied Mathematics, and the National Science Medal in 1999.